to be submitted to APPLIED PHYSICS LETTERS

SAND99-0274J

The band gap of AlGaN alloys

S. R. Lee, A. F. Wright, M. H. Crawford, G. A. Petersen, J. Han, and R. M. Biefeld
Sandia National Laboratories, Albuquerque, NM 87185-0601

(February 1999)

The band gap of $Al_xGa_{1-x}N$ is measured for the composition range $0 \le x < 0.45$; the resulting bowing parameter, b=+0.69 eV, is compared to 20 previous works. A correlation is found between the measured band gaps and the methods used for epitaxial growth of the $Al_xGa_{1-x}N$: directly nucleated or buffered growths of $Al_xGa_{1-x}N$ initiated at temperatures T>800 °C on sapphire usually lead to stronger apparent bowing (b>+1.3 eV); while growths initiated using low-temperature buffers on sapphire, followed by high-temperature growth, lead to weaker bowing (b<+1.3 eV). Extant data suggests that the correct band-gap bowing parameter for $Al_xGa_{1-x}N$ is b=+0.62 (±0.45) eV. © *1999 American Institute of Physics.* [S0000-00000(00)00000-0]

Alloys of the group-III nitrides are increasingly viewed as the materials of choice for implementing detectors, light-emitting diodes, and lasers operating in the ultraviolet. Knowledge of the key properties of these alloys underpins both device development and continued basic studies of these materials. Perhaps the single-most fundamental characteristic of these alloys is their band gap. Widely varying values for the alloy band gaps are reported. For example, we find 20 reports relevant to the band gap of $Al_xGa_{1-x}N$;[1-20] near x=0.5, the high and low reported band gaps span nearly 1 eV. These are amazingly divergent results given that the band gap of GaN at 2 °K has been known to within 3 meV since 1971.[21,22] The purpose of this letter is to clarify the band gap of the AlGaN alloys. We make new measurements of the band gap of nominally unstrained, wurtzite $Al_xGa_{1-x}N$; we compare in detail with previous reports; and we recommend a band-gap bowing parameter based on existing data.

The present experiments used AlGaN alloys grown by metal-organic chemical-vapor deposition (MOCVD) on c-axis sapphire using low-temperature (LT) buffers. The buffers are ~25-nm-thick GaN or AlN grown at 550 °C. Two different types of structures were grown on the LT buffers after ramping to 1050 °C: type-I structures are $Al_xGa_{1-x}N$ single- or multiple-heterolayers of ~1-μm-total thickness grown on ~1-μm-thick GaN; type-II structures are ~1-μm-thick $Al_xGa_{1-x}N$ single-heterolayers grown directly on the buffers. Further growth details are in Ref. 23. Band gaps were determined using photoluminescence (PL) measurements made at 10-295 °K. The samples were excited with the 260-nm output of a frequency-tripled Ti:sapphire laser. The excitation power density was approximately 20 W/cm^2. PL detection was accomplished with a 0.3-meter spectrometer and a UV-enhanced CCD. Biaxial strains and alloy compositions were determined by x-ray diffraction (XRD). (0004) and (20-24) reciprocal-space maps were made using an efficient technique based on position-sensitive x-ray detection.[24] Strained lattice parameters were calculated directly from the paired maps. Compositions, unstrained lattice parameters, and biaxial strains follow using elastic properties given by Wright[25] under the assumption that the unstrained lattice parameters of $Al_xGa_{1-x}N$ vary linearly with x. Rutherford-backscattering spectrometry (RBS) using 2.5 MeV $^4He^+$ or protons was used to verify compositions. Ion-channeling effects in the RBS spectra were randomized by azimuthal rotation of the sample during analysis. AlN mole fractions were extracted from the spectra using the SIMNRA simulation program.[26] We observe XRD compositions that are systematically less than RBS results by $\Delta x \approx -0.09x(1-x)$; this indicates a small, but detectable bowing of the $Al_xGa_{1-x}N$ lattice-parameters with x. The observed composition deviations are marginally greater than the RBS-analysis error (~±0.01) and are consistent within measurement errors with previous observations of a linear relationship between lattice parameters and x.[2,6,9,10]

We report our band-gap measurements for $Al_xGa_{1-x}N$ as an integral part of a dissection of previous works. Parabolic compositional dependence is traditionally assumed for the band gap of alloys: $E_g(x)=f(x)-bx(1-x)$, where the bowing parameter, b, captures the sign and magnitude of the parabolic nonlinearity, and where $f(x)=(1-x)E_g(0)+xE_g(1)$ is simply the linear compositional dependence of the band gap in the absence of bowing. We plot all band-gap results as the deviation of the band gap from linearity: $E_g(x)-f(x)$. The band gaps of unstrained GaN and AlN at 295 °K ($E_g(0)$=3.413 eV[21,22] and $E_g(1)$=6.20 eV[27,28]) are the end-points of our linear benchmark $f(x)$. Suppression of the linear terms illuminates the large differences between reported data sets. Present and previous[1-20] measurements are summarized in this format in Fig. 1. Based on reported details,[1-20] we have applied small nominal corrections to the band gaps bringing all data sets in Fig. 1 to the same reference state: the band gap of unstrained $Al_xGa_{1-x}N$ at ≈295 °K. Corrections were made for band-gap shifts due to: (1) the temperature dependence of the band gap; (2) thermal-expansion-mismatch strain between epilayer and substrate; and (3) epitaxial coherency strain for thin alloy layers grown on thick GaN.

Consider these three corrections in turn. First, various temperature-dependent band-gap shifts between 2 °K and 295 °K are reported for $Al_xGa_{1-x}N$, GaN, and AlN: these shifts span 20-80 meV;[2,22,28] shifts in $Al_xGa_{1-x}N$ do not vary with x.[2] We thus applied a constant -50 meV correction to cryogenic measurements. Second, thermal-expansion-mismatch strains and band-gap shifts are known for GaN; shifts are ≈+12 meV for GaN on sapphire and ≈-7 meV for

DISCLAIMER

GaN on SiC.[29,30] We have calculated shifts for similarly strained $Al_xGa_{1-x}N$ using a Luttinger-Kohn model with crystal-field splittings and deformation potentials derived from density-functional calculations.[31] At fixed thermal-mismatch strain, calculated shifts double as x rises and a valence-band crossover occurs at the minimum of the direct gap; shifts remain <40 meV in magnitude for all x. Third, additional coherency-strain-induced band-gap shifts are important for Refs. 13, 14, and 18; and for partially relaxed type-I structures herein. Strain shifts due to the now-combined effects of epitaxial coherence and thermal mismatch were again calculated; all were <70 meV in magnitude. The uncertainty of the above band-gap shifts are small compared to the large variations between data sets seen in Fig. 1. Thus, temperature-dependent spectral shifts, thermal strains, and coherency strains *are not* explanations for the widely variable results.

We therefore examined the reported details of each work seeking understanding of the observed variations. We found that the data consists of three basic groups: 'Group-A' results report positive deviations of the $Al_xGa_{1-x}N$ band gap from linearity;[7,17,18] 'Group-B' results report negative deviations and $Al_xGa_{1-x}N$ growths conducted on sapphire *without* LT buffers;[1-3,5,6,11,15,19] 'Group-C' results report negative deviations and alloy growths conducted on sapphire *with* LT buffers.[8-10,12-14,16] Group-B also includes one work where $Al_xGa_{1-x}N$ was directly nucleated on SiC at ≈1100 °C,[4] while Group-C includes one work where $Al_xGa_{1-x}N$ was nucleated on optimized GaN on SiC.[20] We now evaluate each group and compare with our results, which fall into Group-C and appear last.

As seen in Fig. 1, Group-A results showing substantial positive deviations of the band gap from linearity are rare. Two of the three results are early works that are now seen to be partly anomalous: Yoshida et al.[17] report very strongly bowed $Al_xGa_{1-x}N$ lattice parameters that deviate by up to ≈-1.1% from present-day values;[2,6,9,10] M. A. Kahn et al.[7] report a band gap for GaN that is 270 meV too high. Both reports raise serious materials-quality issues; the alloys synthesized in these important pioneering works do not appear to give reliable band-gap results. Absent these data, reported band-gap deviations from linearity are predominately negative; bowing is positive.

Group-B alloys, where growths were typically initiated at T>800 °C, usually exhibit stronger bowing (exceptions are Korkotashvili et al.[11] and Zhumakulov[19]): as shown in Fig. 1, most data in this group lie below b=+1.3 eV for x>0.2. Group-B reports tend to exhibit one of two distinct behaviors. The first is *strong quasi-continuous bowing for all x* with b>+1.3 eV as in Fig. 2a.[3,4,6] The second is *initially weak bowing* (b<+1.3 eV for x<0.2) *followed by discontinuous transition* to stronger apparent bowing as in Fig. 2b.[1,2,5,15] Data sets in Fig. 2b are not well described by normal, continuous, parabolic bowing. Instead, the data are better described by weak underlying bowing for all x accompanied by discrete transitions to emission involving sub-gap states. The proposed sub-gap states are deeper in the gap at higher x: emission is 200-400 meV below full-gap for 0.2<x<0.5; the deficit increases to 270-680 meV for x>0.5. Comparing Figs. 2a and 2b, one can see that for x>0.2 the more continuously bowed data of Fig. 2a may involve optical transition via the same sub-gap states shown in Fig. 2b. While observation of dominant sub-gap transitions by emission is common, the sub-gap transitions proposed here are seen by cathodoluminescence (CL)[4,5] and PL,[3] *as well as by* spectroscopic ellipsometry[4,15] and absorption measurements.[1,2,5,6]

In contrast, several groups have performed both optical absorption and PL or CL analyses of $Al_xGa_{1-x}N$ documenting near-band-edge spectral features *concurrent with* strong sub-gap emission.[11,12,16,17,19,32] The sub-gap emission occurs 100-500 meV below full-gap and is observed for 0.1<x<0.8. Earlier work attributes the sub-gap emission to unidentified elemental impurities[11,17,32] acting as acceptors.[32] Recently, Shin et al. attributed these sub-gap transitions to N-vacancy states or other native defects.[12] Robins et al. used backside-illumination PL to observe sub-gap emission from the LT-buffer region of $Al_xGa_{1-x}N$ on sapphire; similar emission is not seen at the top surface. In this case, the sub-gap emission is attributed to extended structural defects or embedded impurity phases in the near-buffer region.[16] No consensus identification emerges, but these reports of sub-gap emission all strongly resemble purported bowing data in Fig. 2. The apparently strong bowing seen for Group-B does seem to arise from incorrectly attributing dominant defect- or impurity-related transitions produced by non-buffered growth to near-edge transitions across the entire gap.

Finally, we come to Group-C results. Alloys grown on both LT-buffers on sapphire, and optimized GaN on SiC, correlate with observations of smaller positive band-gap bowing. In contrast to Group B, Group-C growths all lead to bowing parameters b<+1.3 eV. In Fig. 1, Group-C data partially merge with Group-B data in a zone near b=+1.3 eV for x<0.2, but an important differentiating region exists between 0.2<x<0.45. In this region, Group-B appears to undergo the discontinuous transition to sub-gap emission, while *there is a complete lack of this transition for Group-C.* We attribute the reduced bowing and the lack of sub-gap emission seen for Group-C to reductions in defectivity and/or impurity incorporation -- two-step growth seems to better-minimize unintended sub-gap states allowing one to probe the intrinsic band gap of $Al_xGa_{1-x}N$.

We have fit self-consistent band-gap-bowing parameters to each previous work[1-20] and to this work, which reflect the minor band-gap corrections made herein. We derive a best estimate of the true bowing of unstrained $Al_xGa_{1-x}N$ by simply averaging the fitted bowing parameters for Group-C. The resulting bowing is b=+0.62 (±0.45) eV. Once existing bowing results are filtered to yield those that seem most characteristic of the intrinsic properties of $Al_xGa_{1-x}N$, we find good agreement with our recent density-functional-theory results: b=+0.53 eV.[33] Concluding comparison, we show Fig. 3; present experiments are best fit by a bowing parameter b=+0.69 eV and are consistent with previous Group-C works. Bowing variations within Group-C may be due in part to further variations in materials quality: early two-step growths,[8,9] which used newly invented LT buffers, give stronger bowing than that of recent works,[10,12-14,16,20] where growths benefit from long-term optimization efforts.

Up to this point, we neglect corrections arising from our tentative observation of weak lattice-parameter bowing with

x. Within Group-C, Refs. 12-14, 20, and this work use XRD to determine x. Inclusion of lattice-parameter bowing in the XRD analyses increases x by $\Delta x \approx 0\text{-}0.023$; band-gap deviations accordingly decrease by $-2.79\Delta x$ eV; band-gap bowing increases by $\Delta b \approx 0.1\text{-}0.2$. The net effect is a modest increase in the average band-gap bowing parameter of Group-C to $b=+0.71$ eV. These last corrections are contingent upon the result of further measurements of lattice-parameter bowing in $Al_xGa_{1-x}N$.

The United States Department of Energy supported this work under contract DE-AC04-94AL85000.

[1] O. Ambacher, R. Dimitrov, D. Lentz, T. Metzger, W. Rieger, and M. Stutzmann, J. Cryst. Growth **170,** 335 (1997).
[2] H. Angerer, D. Brunner, F. Freudenberg, O. Ambacher, M. Stutzmann, R. Hopler, T. Metzger, E. Born, G. Dollinger, A. Bergmaier, S. Karsch, and H.-J. Korner, Appl. Phys. Lett. **71,** 1504 (1997); D. Brunner, H. Angerer, E. Bustarret, F. Freudenberg, R. Hopler, R. Dimitrov, O. Ambacher, and M. Stutzmann, J. Appl. Phys. **82,** 5090 (1997).
[3] B. V. Baranov, V. B. Gutan, and U. Zhumakulov, Sov. Phys. Semicond. **16,** 819 (1982); PL data in Fig. 1b are used.
[4] M. D. Bremser, W. G. Perry, T. Zheleva, N. V. Edwards, O. H. Nam, N. Parikh, D. E. Aspnes, and R. F. Davis, MRS Internet J. Nitride Semicond. Res. **1,** 8 (1996).
[5] J. Hagen, R. D. Metcalfe, D. Wickenden, and W. Clark, J. Phys. C **11,** L143 (1978).
[6] T. Huang and J. S. Harris, Appl. Phys. Lett. 72, 1158 (1998).
[7] M. A. Khan, R. A. Skogman, and R. G. Schulze, Appl. Phys. Lett. **43,** 492 (1983).
[8] M. R. H. Khan, Y. Koide, H. Itoh, N. Sawaki, and I. Akasaki, Solid State Comm. **60,** 509 (1986).
[9] Y. Koide, H. Itoh, M. R. H. Khan, K. Hiramatu, N. Sawaki, and I. Akasaki, J. Appl. Phys. **61,** 4540 (1987).
[10] D. Korakakis, H. M. Ng, M. Misra, W. Grieshaber, and T. D. Moustakas, MRS Internet J. Nitride Semicond. Res. **1,** 10 (1996).
[11] G. A. Korkotashvili, A. N. Pikhtin, I. G. Pichugin, and A. M. Tsaregorodtsev, Sov. Phys. Semicond. **18,** 913 (1984).
[12] M. Shin, A. Y. Polyakov, M. Skowronski, D. W. Greve, R. G. Wilson, and J. A. Freitas, Mat. Res. Soc. Symp. Proc. **423,** 643 (1996); A. Y. Polyakov, M. Shin, J. A. Freitas, M. Skowronski, D. W. Greve, and R. G. Wilson, J. Appl. Phys. **80,** 6349 (1996).
[13] G. Steude, D. M. Hofmann, B. K. Meyer, H. Amano, and I. Akasaki, Phys. Stat. Sol. B **205,** R7 (1998).
[14] T. Takeuchi, H. Takeuchi, S. Sota, H. Sakai, H. Amano, and I. Akasaki, Jpn. J. Appl. Phys. **36,** L177 (1997).
[15] T. Wethkamp, K. Wilmers, N. Esser, W. Richter, O. Ambacher, H. Angerer, G. Jungk, R. L. Johnson, and M. Cardona, Thin Solid Films **313,** 745 (1998).
[16] D. K. Wickenden, C. B. Bargeron, W. A. Bryden, J. Miragliotta, and T. J. Kistenmacher, Appl. Phys. Lett. **65,** 2024 (1994); L. H. Robins, J. R. Lowney, and D. K. Wickenden, J. Mater. Res. **13,** 2480 (1998).
[17] S. Yoshida, S. Misawa, and S. Gonda, J. Appl. Phys. **53,** (1982) 6844.
[18] G. Yu, H. Ishikawa, M. Umeno, T. Egawa, J. Watanabe, T. Jimbo, and T. Soga, Appl. Phys. Lett. **72,** 2202 (1998).
[19] U. Zhumakulov, Solid State Comm. **58,** 367 (1986); no data, reports only the bowing parameter, b=0.33 eV, for absorption measurements.
[20] A. S. Zubrilov, D. V. Tsvetkov, V. I. Nikolaev, and I. P. Nikitina, Semiconductors **30,** 1069 (1996).
[21] R. Dingle, D. D. Sell, S. E. Stokowski, and M. Ilegems, Phys. Rev. B **4,** 1211 (1971).
[22] B. Monemar, Phys. Rev. B **10,** 676 (1974).
[23] J. Han, T.-B. Ng, R. M. Biefeld, M. H. Crawford, and D. M. Follstaedt, Appl. Phys. Lett. **71,** 3114 (1997).
[24] S. R. Lee, B. L. Doyle, T. J. Drummond, J. W. Medernach, and R. P. Schneider, in Advances in X-Ray Analysis, Vol. 38, edited by P. Predecki (Plenum Press, NY, 1995) pp. 201-213.
[25] A. F. Wright, J. Appl. Phys. **82,** 2833 (1997).
[26] M. Mayer, SIMNRA User's Guide, Technical Report IPP 9/113, Max-Planck-Institut fur Plasmaphysik, Garching, Germany, 1997.
[27] W. M. Yim, E. J. Stofko, P. J. Zanzucchi, M. Ettenberg, and S. L. Gilbert, J. Appl. Phys. **44,** 292 (1973).
[28] P. B. Perry and R. F. Rutz, Appl. Phys. Lett. **33,** 319 (1978).
[29] H. Amano, K. Hiramatsu, and I. Akasaki, Jpn. J. Appl. Phys. **27,** L1384 (1988).
[30] W. G. Perry, T. Zheleva, M. D. Bremser, R. F. Davis, W. Shan, and J. J. Song, J. Electron. Mat. **26,** 224 (1997).
[31] W. W. Chow, A. F. Wright, A. Girndt, F. Jahnke, and S. W. Koch, Mat. Res. Soc. Symp. Proc. **468,** 487 (1997).
[32] H. G. Lee, M. Gershenzon, and B. L. Goldenberg, J. Electron. Mat. **20,** 621 (1991).
[33] A. F. Wright and J. S. Nelson, Appl. Phys. Lett. **66,** 3051 (1995).

FIG. 1. Measured deviations of the band gap from linearity with x for unstrained $Al_xGa_{1-x}N$ at 295 °K. Dashed line: theoretical bowing by Wright and Nelson.[33] Solid reference lines: $-bx(1-x)$. See also Ref. 19.

FIG. 2. Group-B measurements of the deviation of the band gap from linearity. Characteristic trends seen for $Al_xGa_{1-x}N$ directly nucleated and grown at T>800 °C are: (a) strong quasi-continuous bowing for all x, or (b) weak bowing with discontinuous transition to deeper levels. Solid-black symbols are defined as in Fig. 1.

FIG. 3. Group-C measurements of the deviation of the band gap from linearity. Group-C experiments where $Al_xGa_{1-x}N$ was grown on sapphire by MOCVD using LT buffers are shown.

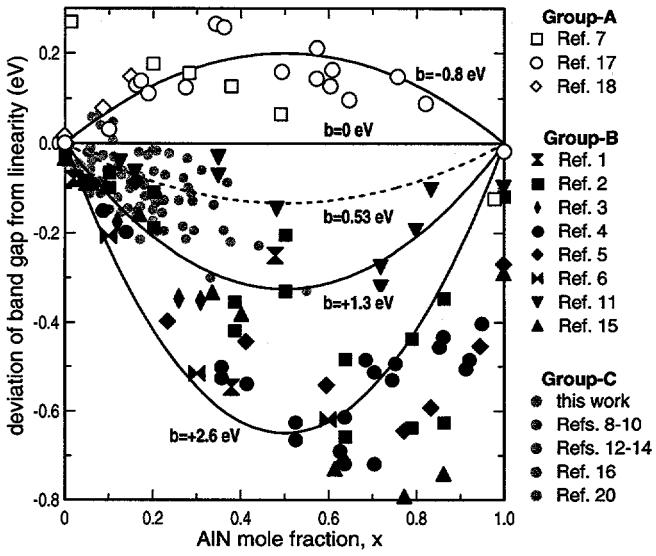

Fig. 1

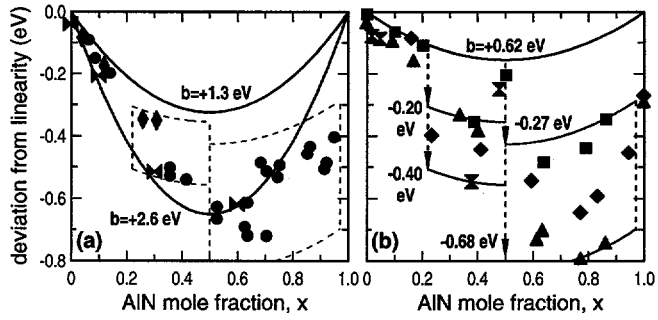

Fig. 2

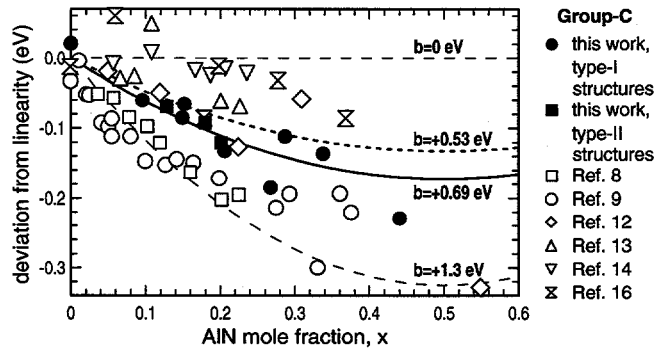

Fig. 3